A domain-transfer support vector machine for multi-temporal remote sensing imagery classification

Conference Paper · July 2017

DOI: 10.1109/IGARSS.2017.8127428

3 authors:

Yiqing Guo
FluroSat Pty LTD

Xiuping Jia
Australian Defence Force Academy

David Paull
UNSW Canberra

A DOMAIN-TRANSFER SUPPORT VECTOR MACHINE FOR MULTI-TEMPORAL REMOTE SENSING IMAGERY CLASSIFICATION

Yiqing Guo[1], Xiuping Jia[1], David Paull[2]

[1]School of Engineering and Information Technology,
The University of New South Wales, Canberra, ACT 2600, Australia
[2]School of Physical, Environmental and Mathematical Sciences,
The University of New South Wales, Canberra, ACT 2600, Australia

ABSTRACT

Multi-temporal remote sensing imagery has become widely available, which opens up an opportunity to improve the efficiency of supervised classification techniques. While a classifier trained from a previous image (source domain) cannot be directly applied to the current image (target domain) because of changes in imaging conditions and dynamics of land surface spectral properties, domain transfer techniques have been introduced in recent years to remove the need for a complete retraining of the current image data. This approach is further developed in the present study, and a domain transfer algorithm named Temporal-Adaptive Support Vector Machine (TASVM) is proposed. The algorithm enables the adaptation of a classifier trained with the source-domain image to the classification of the target-domain image where class data have a different distribution. The adaptation process is allowed to be conducted at the classifier-level where the source classifiers can be transferred without re-accessing the source domain raw data. Experimental analysis showed that the proposed algorithm generated stable results, especially under the circumstances where satisfactory results were hard to achieve with traditional algorithms.

Index Terms— Domain adaptation, knowledge transfer, support vector machines, multi-temporal imagery, remote sensing classification

1. INTRODUCTION

The explosive availability of remote sensing data has challenged the supervised classification methods that require a large number of labelled pixels for every image due to the high cost involved in ground truthing. Multi-temporal remote sensing imagery opens up an opportunity to alleviate this requirement. With domain adaptation techniques, classifiers trained with previous images (source domain) can be transferred to new acquisitions (target domain) without excessive labelling efforts [1]. In other words, the required number of labelled pixels for the classification of target images can be significantly reduced if the assistance from related source classifiers is available [2].

Source classifiers cannot be directly applied to target images because of the existence of cross-domain dataset shift [3] that originates from the following factors. (1) *Covariate Shift*: the source and target class data may follow different probabilistic distributions in the feature space, because of changes in acquisition conditions, within-class variations in spectral characteristics, and temporal dynamics of land surfaces. (2) *Class Imbalance*: the percentage of pixels belonging to a given class may be different between the source and target images. (3) *Class-Set Mismatch*: the source and target images may contain different sets of land cover types. Therefore, an appropriate adaptation strategy needs to be developed to accommodate the cross-domain dataset shift.

Based on the standard support vector machines (SVMs), several adaptation methods have been proposed for solving the domain adaptation problem. However, most of them, such as the Domain Adaptation SVM (DASVM) [1] and the Domain Transfer SVM (DTSVM) [4], rely on the pixels and/or their corresponding labels from the source domain, thus can be categorised as data-level adaptation. In contrast to the data-level adaptation, classifier-level adaptation aims to directly adjust the source classifier into an adapted classifier for the target image without re-accessing the source domain raw data [5]. From a knowledge-transfer perspective, the classifier-level adaptation transfers the summarized knowledge (i.e., the source classifier) instead of raw data (i.e., the pixels and/or their corresponding labels), leading to the following two merits [6]. Firstly, when the size of raw data in the source domain is large, computational load will be greatly reduced if the classifier-level adaptation instead of the data-level adaptation is applied. Secondly, if raw data in the source domain are inaccessible (e.g., private or no longer stored), the classifier-level adaptation is still applicable. Therefore, compared with data-level adaptation, the classifier-level adaptation is more efficient and flexible.

Several classifier-level domain-transfer algorithms have been proposed in the literature [6, 7, 8]. For example, the

Adaptive SVM (ASVM) [7] is able to estimate an adapted target classifier by augmenting a perturbation term to the source classifier [6]. The perturbation term is determined by simultaneously maximizing the similarity of the adapted classifier to the source classifier and minimizing the classification errors on the training pixels in the target domain [6]. However, it has been found that the ASVM tends to generate a small margin space for the adapted target classifier [8]. Another algorithm, PMTSVM [8], is able to estimate an adapted target classifier without penalizing its margin maximization [5]. However, it restricts the included angle between the source and target classifiers to a value equivalent to or less than 90°. This restriction leads to a decreased performance when the underlying optimal target classifier is positioned at an angle greater than 90° from the source classifier. Therefore, considering the limitations of these classifier-level domain-transfer SVMs, improved algorithms still need to be developed to better tackle the problem.

In this study, a new classifier-level domain-transfer algorithm, named Temporal-Adaptive SVM (TASVM), is proposed for cross-domain remote sensing imagery classification. The algorithm synthesizes the source and target domain knowledge as two regularization terms in the objective function, along with a margin-maximization term aimed at maximizing the margin space of the adapted target classifier. Moreover, the source and target classifiers are allowed to be positioned with arbitrary included angles. The adaptation process is allowed to be conducted at the classifier-level where the source classifiers can be transferred without re-accessing the source-domain raw data. In the present study, experiments were conducted on a multi-temporal dataset in order to evaluate the proposed algorithm.

2. PROPOSED ALGORITHM

The proposed TASVM algorithm takes two regularization terms to incorporate the knowledge from both domains: (1) the plenty but inaccurate (with respect to the target-domain classification problem) source-domain knowledge summarized in the source classifier, and (2) the accurate but scarce target-domain knowledge provided by the limited target-domain labelled pixels.

The first regularization term restricts the deviation of the estimated target classifier from the source classifier. In a m-dimensional feature space, the source classifier $f_{\mathrm{s}}(\mathbf{x})$ and target classifier $f_{\mathrm{t}}(\mathbf{x})$ can be expressed as the following respective hyperplanes:

$$f_{\mathrm{s}}(\mathbf{x}) = {\mathbf{w}_{\mathrm{s}}}^{\mathrm{T}}\mathbf{x} + b_{\mathrm{s}}, \tag{1}$$

$$f_{\mathrm{t}}(\mathbf{x}) = {\mathbf{w}_{\mathrm{t}}}^{\mathrm{T}}\mathbf{x} + b_{\mathrm{t}}, \tag{2}$$

where $\mathbf{w}_{\mathrm{s}} = \{w_{\mathrm{s},1}, w_{\mathrm{s},2}, \cdots, w_{\mathrm{s},j}, \cdots, w_{\mathrm{s},m}\}$ and $\mathbf{w}_{\mathrm{t}} = \{w_{\mathrm{t},1}, w_{\mathrm{t},2}, \cdots, w_{\mathrm{t},j}, \cdots, w_{\mathrm{t},m}\}$ are the weight vectors, and b_{s} and b_{t} are the bias factors. To regularize the similarity of the target classifier with the source classifier, a set of slack variables $\boldsymbol{\mu} = \{\mu_1, \mu_2, \cdots, \mu_j, \cdots, \mu_m\}$ are introduced. The elements μ_j restrict the upper and lower bounds of the deviation of $w_{\mathrm{t},j}$ from $w_{\mathrm{s},j}$, resulting in the following respective constraints:

$$-\mu_j \leq w_{\mathrm{t},j} - w_{\mathrm{s},j} \leq \mu_j \text{ and } \mu_j \geq 0, \ \forall j. \tag{3}$$

The second regularization term takes into account the classification error of the estimated target classifier on the labelled target-domain pixels $\mathbf{x}_i$. Similar to those in the standard support vector machines, a set of slack variables ξ_i is used to allow *soft-margin* classification in order to tackle overlapping classes, resulting in the following constraints:

$$y_i\left[{\mathbf{w}_{\mathrm{t}}}^{\mathrm{T}}\mathbf{x}_i + b_{\mathrm{t}}\right] \geq 1 - \xi_i \text{ and } \xi_i \geq 0, \ \forall i, \tag{4}$$

where y_i is the label for $\mathbf{x}_i$. With the expansion of the vectors $\mathbf{w}_{\mathrm{t}}$ and $\mathbf{x}_i$, the constraint in Eq. (4) can be rewritten as:

$$y_i\left[\sum_{j=1}^{m} w_{\mathrm{t},j}x_{i,j} + b_{\mathrm{t}}\right] \geq 1 - \xi_i \text{ and } \xi_i \geq 0, \ \forall i, \tag{5}$$

where $x_{i,j}$ is the jth entry in $\mathbf{x}_i$.

With the constraints in Eqs. (3) and (5), the following optimization problem can be constructed:

$$\begin{aligned} \min_{w_{\mathrm{t},j},\xi_i,\mu_j} \quad & \frac{1}{2}\sum_{j=1}^{m}{w_{\mathrm{t},j}}^2 + C\sum_{i=1}^{n}\xi_i + F\sum_{j=1}^{m}\mu_j \\ \text{s.t.} \quad & y_i\left[\sum_{j=1}^{m} w_{\mathrm{t},j}x_{i,j} + b_{\mathrm{t}}\right] \geq 1 - \xi_i \text{ and } \xi_i \geq 0, \ \forall i, \\ & -\mu_j \leq w_{\mathrm{t},j} - w_{\mathrm{s},j} \leq \mu_j \text{ and } \mu_j \geq 0, \ \forall j, \end{aligned} \tag{6}$$

where n is the number of target-domain labelled pixels. The first term in the objective function $\frac{1}{2}\sum_{j=1}^{m}{w_{\mathrm{t},j}}^2 = \frac{1}{2}\|\mathbf{w}_{\mathrm{t}}\|^2$ accounts for the target-domain margin space. Like that in the standard support vector machines, the term aims to adjust the separating hyperplane to a position that generates the maximum margin space in the target domain. The second and third terms aim to minimze the degree of violation of the constraints, with two positive constants C and F controlling their relative importance in the objective function.

The dual form of the optimization problem in Eq. (6) can be obtained by constructing the following Lagrangian function L:

$$
\begin{aligned}
L =& \frac{1}{2}\sum_{j=1}^{m} {w_{\mathrm{t},j}}^2 + C\sum_{i=1}^{n}\xi_i + F\sum_{j=1}^{m}\mu_j \\
& - \sum_{i=1}^{n}\alpha_i\left[y_i\left(\sum_{j=1}^{m} w_{\mathrm{t},j}x_{i,j} + b_{\mathrm{t}}\right) - (1-\xi_i)\right] \\
& - \sum_{i=1}^{n}\beta_i\xi_i - \sum_{j=1}^{m}\gamma_j\left[\mu_j - (w_{t,j} - w_{s,j})\right] \\
& - \sum_{j=1}^{m}\delta_j\left[(w_{\mathrm{t},j} - w_{\mathrm{s},j}) + \mu_j\right] - \sum_{j=1}^{m}\varepsilon_j\mu_j,
\end{aligned} \tag{7}
$$

where α_i, β_i, γ_j, δ_j, and ε_j are non-negative Lagrange multipliers. Equating the partial derivatives of L to zero with respect to $w_{\mathrm{t},j}$, ξ_i, μ_j, and b_{t} results in the following equations:

$$w_{\mathrm{t},j} - \sum_{i=1}^{n}\alpha_i y_i x_{i,j} + \gamma_j - \delta_j = 0,\ \forall j, \tag{8}$$

$$C - \alpha_i - \beta_i = 0,\ \forall i, \tag{9}$$

$$F - \gamma_j - \delta_j - \varepsilon_j = 0,\ \forall j, \tag{10}$$

$$\sum_{i=1}^{n}\alpha_i y_i = 0. \tag{11}$$

Eliminating $w_{\mathrm{t},j}$, C, F, and b_{t} by substituting Eqs. (8–11) into Eq. (7) results in the following Lagrangian dual function L_{d}:

$$
\begin{aligned}
L_{\mathrm{d}} =& -\frac{1}{2}\sum_{i=1}^{n}\sum_{k=1}^{n}\sum_{j=1}^{m}\alpha_i\alpha_k y_i y_k x_{i,j}x_{k,j} - \frac{1}{2}\sum_{j=1}^{m}{\gamma_j}^2 \\
& - \frac{1}{2}\sum_{j=1}^{m}{\delta_j}^2 + \sum_{i=1}^{n}\sum_{j=1}^{m}\gamma_j\alpha_i y_i x_{i,j} \\
& - \sum_{i=1}^{n}\sum_{j=1}^{m}\delta_j\alpha_i y_i x_{i,j} + \sum_{j=1}^{m}\gamma_j\delta_j \\
& + \sum_{i=1}^{n}\alpha_i - \sum_{j=1}^{m} w_{\mathrm{s},j}\left(\gamma_j - \delta_j\right).
\end{aligned} \tag{12}
$$

Then the following dual optimization problem can be constructed which is equivalent to the primal problem in Eq. (6) but has a simpler form:

$$
\begin{aligned}
\min_{\alpha_i,\gamma_j,\delta_j}\ -L_d \quad \text{s.t. } & 0 \le \alpha_i \le C,\ \forall i, \\
& \gamma_j + \delta_j \le F,\ \gamma_j \ge 0,\ \text{and } \delta_j \ge 0,\ \forall j, \\
& \sum_{i=1}^{n}\alpha_i y_i = 0.
\end{aligned} \tag{13}
$$

Both of the primal and dual problems are quadratic programming problems and can be solved with standard quadratic programming algorithms.

3. EXPERIMENT AND RESULTS

3.1. Experimental Design

The study area was located in southwestern New South Wales, Australia at Coleambally (34°48'S,145°53'E) (Fig. 1a). A total of five land cover classes were identified in the area (Fig. 1b). Two Sentinel-2A optical images acquired on December 05$^{\mathrm{th}}$, 2015 and March 30$^{\mathrm{th}}$, 2016 were used as source-domain and target-domain images, respectively (Figs. 1c and d). Each image consisted of 13 spectral bands covering the visible, near-infrared, and short-wave-infrared spectral regions. In order to better analyze and illustrate the results in a bidimensional feature space, only the Red Band (Band 4; Central Wavelength: 665 nm) and Near-Infrared Band (Band 8; Central Wavelength: 842 nm) were used in the experiment.

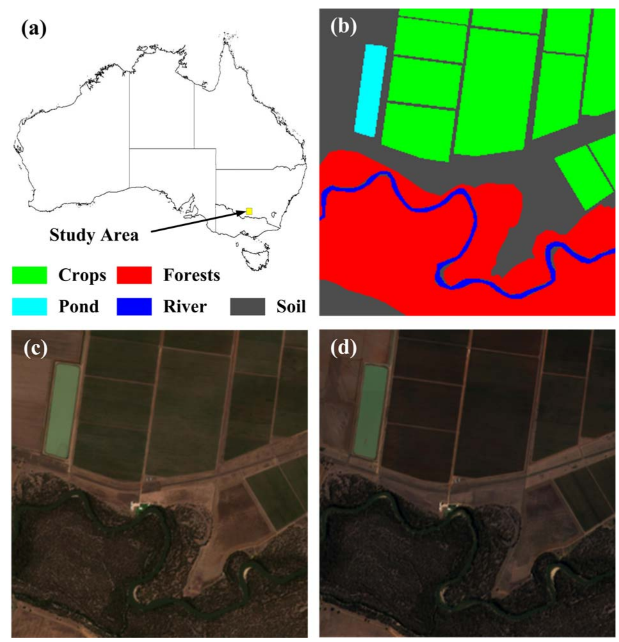

Fig. 1. (a) Study area location; (b) Ground truth map; (c) Source-domain color composite image (Bands 4, 3, and 2) on December 05$^{\mathrm{th}}$, 2015; (d) Target-domain color composite image (Bands 4, 3, and 2) on March 30$^{\mathrm{th}}$, 2016.

The distributions of pixels in the source and target domains are shown in Fig. 2. Compared with other land cover classes, the cross-domain spectral shifts were more obvious for the Crops and Forests. Therefore, cross-domain adaptation of the Crops-against-Forests classifier was considered in the experiment. The cross-domain shifts mainly originated from the different sun-target-sensor geometries and atmospheric conditions, and the phenology of crops and forests. It was assumed that all pixels were labelled in the source domain, while only a few pixels were labelled in the target domain.

In the experiment, a linear classifier $f_{\mathrm{s}}(\mathbf{x})$ separating the

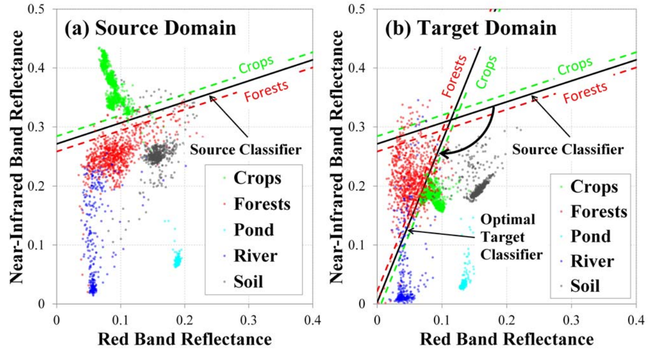

Fig. 2. Distributions of class data shown in a two-dimensional feature space defined by the Red and Near-Infrared Bands, for (a) the source domain and (b) the target domain.

two classes was firstly trained with the source-domain data (Fig. 2a). Then, a set of training data $\{(\mathbf{x}_i, y_i)\}_{i=1}^{\mathcal{N}}$ was randomly selected from the target domain, where $\mathcal{N}$ ranged from two to five with at least one pixel from each class. With the help of $f_{\mathrm{s}}(\mathbf{x})$ and $\{(\mathbf{x}_i, y_i)\}_{i=1}^{\mathcal{N}}$, a target-domain classifier was estimated by the proposed TASVM algorithm. For each $\mathcal{N}$, the procedure was repeated 10000 times with different sets of $\{(\mathbf{x}_i, y_i)\}_{i=1}^{\mathcal{N}}$ being selected. The classification accuracy on the remaining target-domain pixels was used to evaluate the adaptation results. The results achieved by the TASVM algorithm were compared with those obtained by two other classifier-level adaptation algorithms, the ASVM [7] and the PMTSVM [8].

3.2. Results and Discussion

The adaptation performance is shown in Tab. 1. Improvements were observed for the TASVM compared with the ASVM especially with less target-domain labelled pixels. This is because when the number of target-domain labelled pixels is small, the space between the labelled pixels of the two classes tends to be large. The lack of margin maximization in ASVM resulted in biased positions for the estimated target classifiers, leading to a decreased classification result in the target domain. Compared with ASVM and TASVM, PMTSVM presented a considerably poorer performance. This is because the constraint $\mathbf{w}_{\mathrm{s}}{}^{\mathrm{T}}\mathbf{w}_{\mathrm{t}} \geq 0$ adopted in PMTSVM prevented the adaptive target classifier from converging to the underlying optimal target classifier, which is positioned at an obtuse angle (larger than $90°$) with the source classifier as shown in Fig. 2b.

Table 1. Target-domain classification accuracies achieved with different domain transfer algorithms.

Algorithm	Number of Training Samples 2	3	4	5
ASVM	0.68	0.72	0.75	0.77
PMTSVM	0.67	0.62	0.63	0.62
TASVM	0.75	0.78	0.79	0.80

4. CONCLUSION

A domain transfer algorithm named TASVM is proposed for multi-temporal remote sensing imagery classification. The algorithm enables the adaptation of classifiers trained with existing images to new acquisitions where class data have different distributions. Experimental analysis showed that the proposed algorithm generated stable adaptation results, especially under circumstances where satisfactory results were hard to achieve with traditional algorithms.

5. REFERENCES

[1] L. Bruzzone and M. Marconcini, “Domain adaptation problems: A DASVM classification technique and a circular validation strategy,” *IEEE Transactions on Pattern Analysis and Machine Intelligence*, vol. 32, no. 5, pp. 770–787, 2010.

[2] D. Tuia, C. Persello, and L. Bruzzone, “Domain adaptation for the classification of remote sensing data: An overview of recent advances,” *IEEE Geoscience and Remote Sensing Magazine*, vol. 4, no. 2, pp. 41–57, 2016.

[3] J.G. Moreno-Torres, T. Raeder, R. Alaiz-RodríGuez, N.V. Chawla, and F. Herrera, “A unifying view on dataset shift in classification,” *Pattern Recognition*, vol. 45, no. 1, pp. 521–530, 2012.

[4] L. Duan, I.W. Tsang, D. Xu, and S.J. Maybank, “Domain transfer SVM for video concept detection,” in *Computer Vision and Pattern Recognition, 2009. CVPR 2009. IEEE Conference on*. IEEE, 2009, pp. 1375–1381.

[5] L. Shao, F. Zhu, and X. Li, “Transfer learning for visual categorization: A survey,” *IEEE Transactions on Neural Networks and Learning Systems*, vol. 26, no. 5, pp. 1019–1034, 2015.

[6] J. Yang, *Learning to Adapt Across Multimedia Domains*, Ph.D. thesis, Columbia University, 2008.

[7] J. Yang, R. Yan, and A.G. Hauptmann, “Cross-domain video concept detection using adaptive SVMs,” in *Proceedings of the 15th ACM International Conference on Multimedia*. ACM, 2007, pp. 188–197.

[8] Y. Aytar and A. Zisserman, “Tabula rasa: Model transfer for object category detection,” in *2011 International Conference on Computer Vision*. IEEE, 2011, pp. 2252–2259.